Biological and Chemical Gold Nanosensors based on Localized Surface Plasmon Resonance

Grégory Barbillon, Jean-Louis Bijeon, Jérôme Plain, Marc Lamy de la Chapelle, Pierre-Michel Adam and Pascal Royer

Institut Charles Delaunay-Université de Technologie de Troyes, CNRS FRE 2848-Laboratoire de Nanotechnologie et d'Instrumentation Optique (LNIO), 12 rue Marie Curie BP2060, 10010 Troyes Cédex, France
E-mail: bijeon@utt.fr
Tél: 33 3 25 71 56 62, Fax: 33 3 25 71 84 56

Abstract

In this paper, we discuss the performances of gold nanosensors based on Localized Surface Plasmon Resonance (LSPR) designed by Electron Beam Lithography (EBL) in the context of biological and chemical sensing. We demonstrate the sensitivity of our gold nanosensors by studying the influence of the concentration of 11-mercaptoundecanoic acid (MUA) on the shift of LSPR wavelength. Additionally, to study the selectivity of our nanosensors, the system Biotin/Streptavidin was used to detect very weak concentration of biomolecules. These results represent new steps for applications in chemical research and medical diagnostics.

1 Introduction

Advancements in nanotechnology due to a better knowledge of chemical and physical properties of materials enable new developments of biological and chemical nanosensors. The improved chemosensors (1-6) and biosensors (7-11) are based on the extraordinary optical properties of noble metal nanoparticles. Indeed, the LSPR nanosensors induce the small local refractive index changes at the surface of metallic nanoparticles (5,12). The nanosensors based on LSPR spectroscopy operate in a manner totally analogous to propagating surface plasmon resonance (SPR) sensors. That is by transducing small changes in the refractive index near the metallic surface into a measurable wavelength shift response. Variations of the reflectivity as a function of the angle of incidence in SPR and extinction peaks in LSPR are related to the same physical phenomena, collective oscillation of electrons in the metal. The minimum of reflection corresponds to a maximum of absorption. The response of LSPR and SPR sensors can be described by the following formula (12,13):

$$\Delta\lambda_{max} = m\Delta n[1-\exp(\frac{-2d}{l_d})]\qquad(1)$$

where $\Delta\lambda_{max}$ is the wavelength shift, m is the refractive index sensitivity, Δn is the change in refractive index induced by an adsorbate, d is the effective adsorbate layer thickness and l_d is the characteristic evanescent electromagnetic field decay length. This equation can be applied for both SPR and LSPR, because they are intrinsically related to the same physical phenomena, the only differences are the propagating length of the surface Plasmon, which is of 10 μm order for the SPR and only about 10 nm order for LSPR, and the decay length which is much smaller for LSPR than for SPR. This model assumes a single exponential decay of the electromagnetic field normal to the planar surface, which is a simplification for the electromagnetic fields associated with metallic nanoparticles. This simplified model enables us to optimize the response of our LSPR nanosensors. The m factor for SPR sensors is about 2×10^6 nm/RIU (13) (Refractive Index Units) and is about 2×10^2 nm/RIU (14) for LSPR sensors, this difference is largely compensated by the very low decay length offered by LSPR gold nanoparticle. Indeed this decay length is around 200-300 nm (14) for SPR sensors whereas is few nanometers (14) for LSPR nanosensors (for our Au nanoparticles l_d = 15 nm). This decay length depends on the size, shape, and composition of the nanoparticles and gives rise to the large sensitivity of the LSPR nanosensor. This low decay length permits to detect a very thin layer of adsorbate molecules. Even if the sensitivity of the SPR sensors is slightly better than that of LSPR nanosensors, a direct comparison is not evident because of the different mechanisms that give rise to their respective sensitivity gains. Nevertheless some advantages of LSPR nanosensors could be mentioned. The LSPR nanosensors do not require a temperature control compared to SPR since the large refractive index sensitivity of SPR induces a strong dependence on the environmental temperature. No
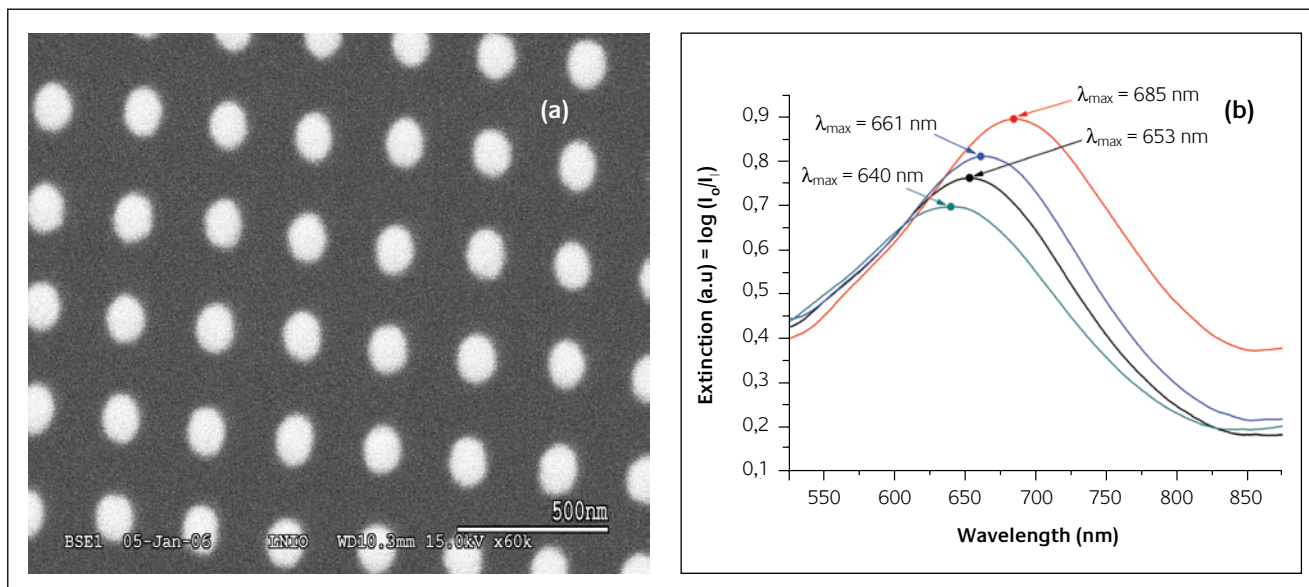
Figure 1

(a) SEM image of Au nanoparticles and (b) example of obtained extinction spectra after each functionalization step (Au +MUA+biotin+SA)

specific angular conditions of excitation are required for LSPR, no needs of prism coupler-based, grating coupler-based or optical waveguide. In practice SPR sensors require at least 10x10 μm^2 area for sensing experiment, whereas for LSPR sensing the probed zone can be minimized to a large number of individual sensing elements up to a single nanoparticle using confocal or near-field measurement techniques. Finally the extinction spectroscopy does not need a complex device; a UV-visible microspectrometer can be efficient enough to get the spectra.

In this paper, the sensitivity of Au nanoparticles to their dielectric environment will be studied for the detection of MUA and Streptavidin. Additionally, the selectivity of our system is studied while varying the concentration of Streptavidin in the system Biotin/Streptavidin.

2   Experimental methods

Metallic nanoparticles preparation
We use the Electron Beam Lithography (EBL) for the fabrication of these nanosensors. The EBL system permits to control with high precision the shape, the size, but also the distance between the nanoparticles and consequently to tune LSP resonance of metallic nanoparticles arrays (15-17) on the whole visible range. Thus we can choose the spectral band which appears to be the most sensitive to the adsorption of chemical and biological molecules. The obtained metallic nanocylinders have in plane diameters of 100 nm and a 200 nm fixed interparticle distance as determined by SEM, see figure (1(a)) and out of plane mean heights of 50 nm as checked by Atomic Force Microscopy (AFM). The interparticle distance is large enough to avoid an electromagnetic coupling between the particle and each particle can be considered as individual (16).

Optical characterisation

Visible extinction spectra were measured using a Jobin Yvon micro-Raman Spectrometer (Labram) in standard transmission geometry with unpolarized white light. The transmitted light is collected by an objective (x10; N.A = 0.25) on a real area of 30x30μm^2. The extinction spectra were used to determine the position of the localized surface plasmon resonance and its shift after adsorption of molecules. All measurements were collected in air and to prevent atmospheric contamination, they have been performed on freshly prepared samples.

Materials
11-Mercaptoundecanoic acid (MUA), Streptavidin (SA), Biotin ethylenediamine, 1-Ethyl-(3-dimethylaminopropyl) Carbodiimide hydrochloride (EDC), 10mM and 20mM phosphate buffered saline (PBS) were purchased from Sigma-Aldrich.

3   Results and discussion

The Au/MUA and Biotin/SA systems which we used will illustrate the properties of our LSPR nanosensors. We can simply model the systems curves by the following formula (12)

$$\Delta\lambda = \Delta\lambda_{max} \left(\frac{K_{a,surf} [Analyte]}{(1+K_{a,surf} [Analyte])} \right) \quad (2)$$

where $\Delta\lambda$ is the nanosensor response for a given MUA or SA concentration, $\Delta\lambda_{max}$ (in our case 32.8 nm for MUA and 28 nm for SA) is the maximum response of studied system and $K_{a,surf}$ is the surface confined binding constant of the same system and [Analyte] is the concentration of MUA or SA.

The binding between MUA and Au
The samples were prepared by immersion in a given concentration of MUA in ethanol at room temperature for 24 hours. The LSPR λ_{max} shift, $\Delta\lambda$, versus the [MUA] concentration
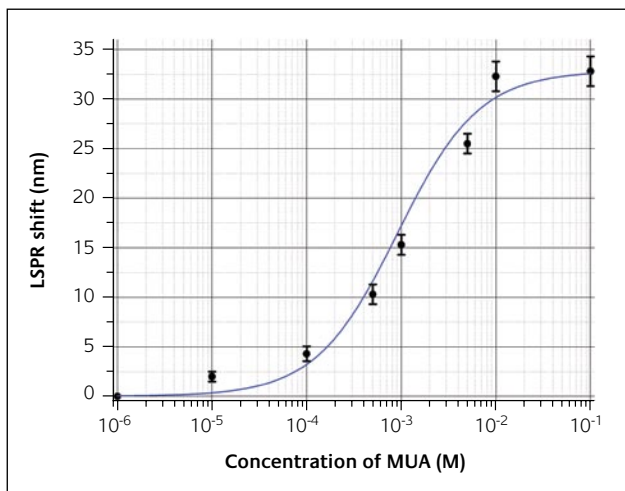
Figure 2

The specific binding of MUA to an Au nanosensor is shown in the response curve. The solid line is the calculated value of the nanosensor response from equation (2)

Figure 3

The specific binding of SA to biotin is shown in the response curve. The solid line is the calculated value of the nanosensor response from equation (2)

response curve was measured over the range 10^{-6} M < [MUA] < 10^{-1} M (figure (2)). Each data point is an average resulting from the analysis of eight identical samples under the same conditions. According to figure 2, the limit of detection (LOD) is 10μM for MUA. From the binding curve, we can calculate the surface-confined binding constant $K_{a,surf}$ and we obtained $(1.1\pm0.2)10^3$ M^{-1} for 11-mercaptoundecanoic acid. This value is directly correlated to an important characteristic of the system: the limit of detection (LOD). It means that the larger the binding constant $K_{a,surf}$ is the weaker the LOD becomes and inversely. From equation (1), we can obtain the total number of molecules of MUA on real probed zone ($30 \times 30 \mu m^2$). At the LOD, it corresponds to 1.13×10^8 molecules (1.88×10^{-16} mol) corresponding to a density of 11300 MUA molecules per nanoparticle. We have then a very sensitive system of detection, even if the MUA is a small molecule (218 AMU: Atomic Mass Units). Consequently we can get a much better LOD for larger molecules as it will be shown in the next section.

Monitoring the specific binding of Streptavidin to Biotin

This Biotin/SA system was selected for its high binding affinity ($K_a \sim 10^{13}$ M^{-1}) and will serve as a very good model for the LSPR nanosensor. The Streptavidin is a tetrameric protein and can bind to four biotinylated molecules (antibodies, nucleic acids, etc.) by modifying very little their biological activity. The LSPR nanosensors are prepared for biosensing events in the following way. The Au nanocylinders are first functionalized with MUA (1mM) in ethanol during 24 hours. Next, biotin was covalently attached to the carboxylate groups via incubation in a 1:1 ratio of EDC:biotin (concentration of biotin: 1 mM) in 10 mM PBS during 3 hours. To finish, the samples were incubated in a given concentration of SA in PBS for 3 hours. We rinsed with much attention our samples with 10 mM and 20 mM PBS after biotinylation and detection of SA to remove the non-specifically bound materials.

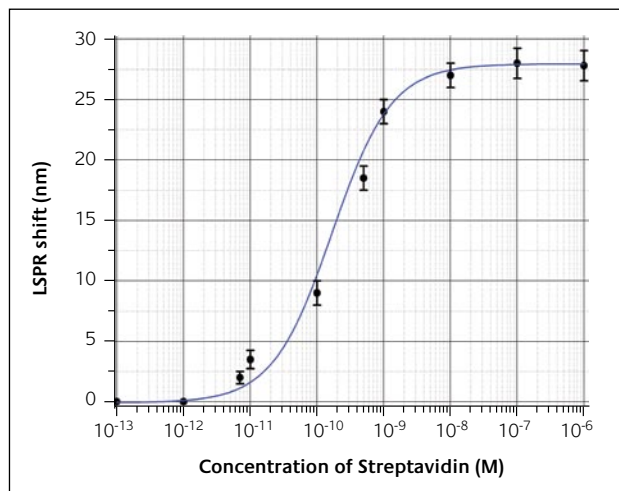For the monitoring of the specific binding between the

biotin and the SA, we varied the concentration of SA between 10^{-13} M and 10^{-6} M and we measured respectively the shift of LSPR wavelength after adsorption of SA (figure 3). We found the LOD of this system which is 7 pM. As previously we also calculated the $K_{a,surf}$ value and we obtained $(6.1 \pm 0.3) 10^9$ M^{-1} for the Biotin/SA system.

We can calculate the number of molecules of SA. From equation (1), we first deduced by a simple calculation (18) the number of molecules of MUA per nanoparticle and we found 30000 molecules (for 1mM of MUA concentration). Then the effectiveness (19) of the binding Biotin/MUA is about 1-5% that gives us 300-1500 biotin sites per nanoparticle, this number is determined by the yield of the EDC coupling reaction. Thus we can estimate at the LOD the smallest number of molecules of SA per nanoparticle which is 75 (1 SA for 4 Biotin) corresponding to 1.25×10^{-22} mol. Moreover we can estimate the total number of probed molecules of SA to be 7.5×10^5 (probed zone: $30 \times 30 \mu m^2$).

4 Conclusions

Our results suggest that Au nanocylinder sensors could be used, in the near future, for the detection of a wide variety of chemical and biological molecules.

In this study, we report the use of Au nanoparticles, fabricated using EBL, as nanosensors to probe the interaction between Au and MUA in solution, and the binding between Biotin and Streptavidin. The maximum LSPR wavelength shifts observed for MUA and SA were respectively $\Delta\lambda_{max}$ = 32.8 nm and 28 nm. We noted that the surface binding affinity is $(1.1\pm0.2)10^3$ M^{-1} for the binding of MUA to Au nanoparticles and $(6.1\pm0.3) 10^9$ M^{-1} for the binding between Biotin and Streptavidin. Also, the limit of detection for the nanosensor was determined to be 1.88×10^{-16} mol for MUA and 1.25×10^{-18} mol for SA, corresponding to a density of respectively 11300 MUA and 75 SA per nanoparticle. The total number of probed molecules is

1.13×10^8 for MUA and 7.5×10^5 for SA, with a probed zone of $30 \times 30 \ \mu m^2$.

Although the results presented in this work are far from conclusive, the advantages of LSPR-based sensors discussed in the introduction open the possibilities of further developments in a wide range of chemical and medical applications.

Acknowledgements

About the authors

Grégory Barbillon completed his PhD in Physics (2007) at the University of Technology of Troyes under the supervision of Prof. J.-L. Bijeon. Then he was awarded a post-doc position at the University of Lyon. In recent years, his interest were focused on plasmonics, the fabrication and the study of biological and chemical nanosensors based on localized surface plasmon resonance, the scanning near-field optical microscopy and the luminescence of nanoparticles.

Jean-Louis Bijeon is associate professor at University of Technology of Troyes, he is the Head of the Physics, Materials and Nanotechnology department. He got his PhD from University of Burgundy (France) and from Oak Ridge National Laboratory (USA) in 1989 on Surface Enhanced Raman Scattering and its relations with the Localized Surface Plasmon Resonance on submicronic metallic particles. He was the R&D project manager, in scanning tunnelling microscopy and photon scanning tunnelling microscopy at SPIRAL R&D a French private company, from January 1990 to February 1994. Now its research themes inside the Nanotechnology and Optical Instrumentation Laboratory at UTT, are near-field optics and related fields involving surface plasmon resonance in metallic nanoparticles, and plasmonics. Another field of its activities is the expertise in atomic force microscopy.

Jérôme Plain gratuated in Physics (1998) and completed his PhD (europeus doctor) in Physics (2001) at the Université of Poitiers and the Autonomous University of Barcelona. He is now assistant professor of physics at the University of Technology of Troyes. In recent years, his interests were mainly focused on metal nanostructures and their applications.

Marc Lamy de la Chapelle got is PhD in 1998 on the Raman spectroscopy of carbon nanotubes. Since 2001, he was assistant professor at the University of Technology of Troyes. He is specialized in the vibrational spectroscopies and more especially on the Surface Enhanced Raman Scattering. He was recently promoted Professor at the University of Paris 13 working on the application of SERS to the characterisation of biological structures.

Pierre-Michel Adam has obtained his PhD thesis in January 95 at the University of Burgundy (France). In january 95, Pierre Michel Adam has joined the University of Technology of Troyes as an assistant professor and has been appointed professor since february 2003. His fields of research are near-field microscopy and spectroscopy (fluorescence, absorption), surface plasmons, surface enhanced Raman scattering.

Pascal Royer is a full Professor in Physics at the University of Technology of Troyes (UTT). He has a background in physics and particularly in optics/optoelectronics, graduated in Dijon (PhD) and Grenoble (HDR). He is the Director of the Nanotechnology and Optical Instrumentation Laboratory he founded at UTT in 1994. These scientific investigations concern the study of physical/chemical properties of nanostructures by near field optical microscopy and spectroscopy so as the development of related instrumentation and the understanding of physical phenomena involved at this scale. He has also always been involved in plasmonics.

References

1   U. Kreibig, M. Gartz and A. Hilger, *Ber. Bunsen-Ges,* 1997, 101, pp. 1593-1604

2   G. Kalyuzhny, A. Vaskevick, G. Ashkenasy and A. Shanzer, *J. Phys. Chem. B,* 2000, **104**, pp. 8238-8244

3   M. Sanekata and I. Suzuka, *Chem. Phys. Lett,* 2000, **323**, pp. 98-104.

4   G. Kalyuzhny, M. A. Schneeweiss, A. Shanzer, A. Vaskevick and I. Rubinstein, *J. Am. Chem. Soc,* 2001, **123**, pp. 3177-3178

5   M. D. Malinsky, K. L. Kelly, G. C. Schatz and R. P. Van Duyne, *J. Am. Chem. Soc,* 2001, **123**, pp. 1471-1482

6   A. Henglein and D. Meisel, *J. Phys. Chem. B,* 1998, **102**, pp. 8364-8366

7   C. A. Mirkin, R. L. Letsinger, R. C. Mucic and J. J. Storhoff, **Nature**, 1996, **382**, pp. 607-609

8   H. Takei, Proc. *SPIE-Int. Soc. Opt. Eng,* 1998, **3515**, pp. 278-283

9   S. Connolly, S.Cobbe and D. Fitzmaurice, *J. Phys. Chem. B,* 2001, **105**, pp. 2222-2226

10 C. L. Haynes and R. P. Van Duyne, *J. Phys. Chem. B,* 2001, **105**, pp. 5599-5611

11 R. Elghanian, J. J. Storhoff, R. C. Mucic, R. L. Letsinger and C. A. Mirkin, *Science,* 1997, **227**, pp. 1078-1080

12 J. C. Riboh, A. J. Haes, A. D. McFarland, C. R. Yonzon and R. P. Van Duyne, *J. Phys. Chem. B,* 2003, **107**, pp. 1772-1780

13 L. S. Jung, C. T. Campbell, T. M. Chinowsky, M. N. Mar, S. S. Yee, *Langmuir* 1998, **14**, 5636-5648

14 D. A. Stuart, A. J. Haes, C. R. Yonzon, E. M. Hicks and R. P. Van Duyne, *IEE Proc.-Nanobiothecnol.,* February 2005, Vol. 152, No. 1

15 J. Grand, M. Lamy de la Chapelle, J.-L. Bijeon, P.-M. Adam, A. Vial, and P. Royer, *Phys. Rev. B,* 2005, (**72/3**), 033407

16 J. Grand, S. Kostcheev, J.-L. Bijeon, M. Lamy de la Chapelle, P.-M. Adam, A. Rumyantseva, G. Lérondel, P. Royer, *Synth. Met.,* 2003, **139**(3), 621-4

17 L. Zhao, K. L. Kelly and G. C. Schatz, *J. Phys. Chem. B,* 2003, **107**, 7343

18 F. Schreiber, *Progress in Surface Science* 2000, **65**, pp. 151-256

19 G. T. Hermanson, *Bioconjugate Techniques,* 1996